Available online at www.sciencedirect.com

SCIENCE DIRECT

Developmental Biology 285 (2005) 224 – 237

DEVELOPMENTAL BIOLOGY

www.elsevier.com/locate/ydbio

The control of morphogen signalling: Regulation of the synthesis and catabolism of retinoic acid in the developing embryo

Susan Reijntjes, Aida Blentic, Emily Gale, Malcolm Maden*

MRC Centre for Developmental Neurobiology, 4th floor New Hunt's House, King's College London, Guy's Campus, London Bridge, London SE1 1UL, UK

Received for publication 15 March 2005, revised 18 May 2005, accepted 10 June 2005
Available online 27 July 2005

Abstract

We consider here how morphogenetic signals involving retinoic acid (RA) are switched on and off in the light of positive and negative feedback controls which operate in other embryonic signalling systems. Switching on the RA signal involves the synthetic retinaldehyde dehydrogenase (RALDH) enzymes and it is currently thought that switching off the RA signal involves the CYP26 enzymes which catabolise RA. We have tested whether these enzymes are regulated by the presence or absence of all-*trans*-RA using the vitamin A-deficient quail model system and the application of excess retinoids on beads to various locations within the embryo. The *Raldhs* are unaffected either by the absence or presence of excess RA, whereas the *Cyp*s are strongly affected. In the absence of RA some, but not all domains of *Cyp26A1*, *Cyp26B1* and *Cyp26C1* are down-regulated, in particular the spinal cord (*Cyp26A1*), the heart and developing vasculature (*Cyp26B1*) and the rhombomeres (*Cyp26C1*). In the presence of excess RA, the *Cyp*s show a differential regulation-*Cyp26A1* and *Cyp26B1* are up-regulated whereas *Cyp26C1* is down-regulated. We tested whether the Cyp products have a similar influence on these genes and indeed 4-*oxo*-RA, 4-OH-RA and 5,6-*epoxy*-RA do. Furthermore, these 3 metabolites are biologically active in that they fully rescue the vitamin A-deficient quail embryo. Finally, by using retinoic acid receptor selective agonists we show that these compounds regulate the *Cyp*s through the RARα receptor. These results are discussed with regard to positive and negative feedback controls in developing systems.

Keywords: Morphogen; Catabolism; Retinoic acid; RAR; Cyp26; Raldh

Introduction

The identification of morphogens or signalling molecules and elaborating how and where they act in the embryo is one of the most intriguing aspects of developmental biology. Initially, the mere identification of these signalling molecules—retinoic acid (RA), sonic hedgehog (Shh), fibroblast growth factor (FGF), Wnts, bone morphogenetic proteins (BMPs) was a major advance and this was subsequently followed by the discovery of their pathways of action between cells and within the cell. As more has been revealed about the cellular components of a morphogenetic signal, it has become clear that once such a signal has been turned on, temporal regulation becomes important and the signal subsequently needs to be turned off. This has led to the identification of morphogen antagonists.

There are several ways in which this temporal regulation could be controlled, the most obvious would be by transcriptional or translational control of the morphogen, but this seems not to be the preferred way. Instead, another factor, an antagonist, is synthesised which interferes with or destroys the morphogen. For example, the action of the Wnt proteins are inhibited either by direct binding to secreted frizzled-related protein or Wnt inhibitory factor, or the Wnt inhibitors Dickkopf and Wise bind to the Wnt co-receptors resulting in their removal from the cell surface by internalisation making them unavailable for Wnt reception (Logan and Nusse, 2004). Similarly, in the Shh pathway Hip1 and Gas1 are proteins localised at the plasma membrane that

* Corresponding author. Fax: +44 207 848 6798.
E-mail address: malcolm.maden@kcl.ac.uk (M. Maden).

0012-1606/$ - see front matter © 2005 Elsevier Inc. All rights reserved.
doi:10.1016/j.ydbio.2005.06.019

bind Shh and attenuate signalling and in addition Rab23 may inhibit Shh by regulating endocytosis or vesicle transport of Ptc1, the cell surface receptor (Cohen, 2003; Evans et al., 2003; Eggenschwiler et al., 2001). BMP signalling is inhibited primarily by molecules such as chordin, noggin and follistatin binding BMP ligands in the extracellular space and preventing them interacting with the cell surface receptors. In addition, there is competition between the Smads in the cytosol and the ubiquitin ligases Smurf1 and -2 target Smad1, Smad2 and the cell surface receptors for degradation by the proteosomes (Munoz-Sanjuan and Brivanlou, 2002). Fibroblast growth factor (FGF) signalling through its receptor tyrosine kinase is inhibited by the *sprouty* gene family. The FGF signal is transmitted inside the cell through the Ras/Raf/MAPK pathway resulting in ERK activation and sprouty acts by direct binding to these signalling components (Kim and Bar-Sagi, 2004). These negative feedback systems are widespread in development because they generate stability when confronted with environmental fluctuations (Freeman, 2000). Conversely, positive feedback loops are normally considered to generate instability even though there are examples of this within the pathways discussed above as well as others (Freeman, 2000). It is therefore of interest to examine the feedback systems which operate in the RA signalling system.

RA is a low molecular weight (300 Da), lipophilic, rapidly diffusing signalling molecule which acts directly on the nucleus to activate gene expression via heterodimerisation of the nuclear transcription factors, the retinoic acid receptors (RARs), and the retinoid X receptors (RXRs) (Chambon, 1996). The 'on' signal for RA is its localised synthesis from retinol via retinal using the retinaldehyde dehydrogenase enzymes (RALDHs) which oxidise retinal to all-*trans*-RA (Duester, 1996, 2000). The 'off' signal is considered to be the catabolism of all-*trans*-RA by the action of 3 cytochrome P450 enzymes (CYPs), to products such as 4-*oxo*-RA, 4-OH-RA and 18-OH-RA (Fujii et al., 1997; White et al., 1997, 2000). Therefore, one of the keys to understanding the action of RA is to identify where and when RA is synthesised and catabolised in the embryo by examining the distribution of these enzymes and to determine how these enzymes are regulated by their substrates.

So far, the distribution of three RALDHs, RALDH1, RALDH2 and RALDH3 and three CYPs, CYP26A1, CYP26B1 and CYP26C1 have been described in the developing embryo. These expression patterns have revealed a level of subtlety that is not obvious using other means of identifying RA sites of action. For example, in mouse and chick embryos, *Raldh1* is expressed relatively late in development and in very restricted regions such as the dorsal neural retina of the eye and the mesonephros (McCaffery et al., 1991; Blentic et al., 2003).

All embryos studied express *Raldh2* and it appears soon after gastrulation when it is expressed in the newly generated mesenchyme (Berggren et al., 1999; Niederreither et al., 1997; Swindell et al., 1999). As development proceeds *Raldh2* remains in the mesenchyme of the somites and lateral plate, and additionally is expressed in the heart (Moss et al., 1998) and nephrogenic mesenchyme. In mouse and chick there is little expression of *Raldh2* in the head of the embryo apart from the eye and an area of mesenchyme caudal to the eye (Blentic et al., 2003). Later, it is expressed in the meninges around the spinal cord and in the motorneurons and the roof plate within the spinal cord (Zhao et al., 1996). In chick, *Raldh3* is expressed in very discrete locations such as the stage 4 Hensen's node, the endoderm at the edge of the neural plate below the developing heart (Blentic et al., 2003). In chick and mouse, expression of Raldh3 continues in the epithelium abutting the developing forebrain (Schneider et al., 2001), the ventral half of the developing eye, the dorsal part of the otic vesicle, Rathke's pouch and a stripe at the midbrain/hindbrain border (Li et al., 2000; Mic et al., 2000).

Cyp26A1 has a fascinating expression pattern which in some regions is complementary to *Raldh2*. Expression begins at the same time as *Raldh2*, but in a region at the anterior end of the embryo which is the presumptive forebrain and midbrain neurectoderm (de Roos et al., 1999; Fujii et al., 1997; Swindell et al., 1999). In the chick embryo, it then becomes restricted to the anterior neural folds, rhombomere 3 in the hindbrain, an equatorial region of the eye or the dorsal lens and the dorsal third of the anterior spinal cord. At the posterior end of the embryo, there is another domain of *Cyp26A1* in the tail bud and hindgut. *Cyp26B1* is expressed in the developing vasculature, the heart and the distal mesenchyme of the progress zone of mouse and chick embryos (MacLean et al., 2001; Reijntjes et al., 2003). In the chick hindbrain, it has a very intriguing expression pattern in subsets of neurons within rhombomeres 2, 4 and 6 and in rhombomere 1 which contributes to the cerebellum (Reijntjes et al., 2003). In the chick, *Cyp26C1* is expressed in the anterior mesenchyme and may act as the 'sink' to *Raldh2* which is the 'source' of RA in the posterior mesenchyme in the early embryo, these two together may help to pattern the overlying neural plate (Reijntjes et al., 2004). Subsequently, *Cyp26C1* is localised to the head in the neural crest from anterior rhombomeres, domains of cranial mesenchyme, dynamically in the rhombomeres and in mouse, the inner ear and tooth buds (Tahayato et al., 2003).

In the work described here, we have considered whether the *Raldh*s and the *Cyp*s are affected by the presence or absence of RA and the Cyp products. To perform this, we have, on one hand, used the vitamin A-deficient (VAD) quail model which develops in the absence of detectable RA, and on the other hand, we have added RA and other retinoids on beads to various areas of the chick embryo where these enzymes are expressed. We find that the *Raldh*s are minimally affected by the presence or absence of RA, whereas the *Cyp*s are dramatically affected both by their

substrate, RA and their catabolic products leading to a situation involving positive feedback and resultant degradation of the RA signal. However, we also show that the *Cyp* catabolic products are themselves biologically active which considerably complicates the role of the Cyp enzymes in RA signalling in the embryo.

Materials and methods

Embryos

Vitamin A-deficient (VAD) embryos were obtained from a colony of quails kept at King's College London. The breeding quails are fed on a defined retinoid free diet with 10 mg kg^{-1} of all-*trans* RA as the only source of vitamin A in order to permit fertilisation. As RA cannot be detected in the VAD embryo either by HPLC (Dong and Zile, 1995), by a F9 reporter cell line (Chen et al., 1995) or by lack of immunoreactivity with a specific anti-RA monoclonal antibody (Twal et al., 1995), these embryos are effectively RA free. The VAD embryos and fertilised hens' eggs (mixed flock, Henry Stewart and Co. Ltd., Louth, Lincolnshire) were incubated in a humidified atmosphere at 37°C. Embryos were staged according to Hamburger and Hamilton (Hamburger and Hamilton, 1951).

Whole-mount in situ hybridisation

Digoxigenin (Roche) labelled antisense RNA probes for *Cyp26B1* and *Cyp26C1* were prepared as described previously (Reijntjes et al., 2003, 2004). Other probes were kindly given by E. Swindell (*Cyp26A1*), R. Godbout (*Raldh1*) and F. Grun (*Raldh3*). *Raldh2* was prepared as described previously (Blentic et al., 2003). Whole-mount in situ hybridisation was carried out using standard procedures, prehybridisation and hybridisation was carried out at 70°C with a probe concentration of 1 μg/ml and visualised with digoxigenin antibodies conjugated to alkaline phosphatase reacted with NBT/BCIP purple (Roche) to give a purple colour reaction.

Vibratome sectioning of stained embryos

Embryos were embedded in 3.6 ml vibratome embedding mix (gelatine type A, egg albumin, Sigma, sucrose, BDH), incubated for 2 h at room temperature and then 400 μl glutaldehyde (Sigma) was added. Sections were cut at 80 μm on a vibratome (Leica VT 1000S), placed on glass microscope slides and mounted in glycerol.

Anion exchange resin bead analysis

All-*trans*-RA (obtained from Sigma), 5,6-epoxy-RA, 4-*oxo*-RA and 4-OH-RA (Hoffmann-La Roche, Basel), CD336, CD2019 and CD437 (a kind gift of Galderma, Sofia Antipolis) compounds were dissolved in 250 μl dimethyl sulfoxide (Sigma-Aldrich, USA) to a concentration of 4 mg/ml, placed in a 1.5-ml Eppendorf and analytical grade anion exchange resin beads AGI-X2, 100–200 Mesh Formate Form (Bio-RAD) added. Excess retinoid solution was removed and to visualise the beads 1 ml of Dulbecco's MOD Eagle Medium (Gibco) was added. Part of the vitilline membrane was carefully removed from stage 9 embryos and 1–3 beads placed either by the head or posterior trunk. The embryos were then incubated for 24 h at 37°C. Before dissection into PBS and fixation in 4% paraformaldehyde, the position of the beads relative to the embryo was noted.

Cultures

The hindbrain region of the embryo (including branchial arches and mesenchyme) and tail bud were dissected from stage 8 to 10 embryos and cultured in collagen matrix (ICN Flow), prepared by mixing 1 volume of 7.5% sodium bicarbonate, 1 volume of 10× medium (DMEM, Gibco) and eight parts collagen. The pH was adjusted to 7.5 by dropwise addition of NaOH. The medium consisted of DMEM-F12 with glutamine (Gibco), 6% glucose, GMS-A (a trace element mixture of insulin, transferring and selenium, Gibco) and all-*trans*-RA (stock solution 1×10^{-6} M, Sigma). Explants were cultured overnight.

Semiquantitative reverse transcription-PCR analysis

RNA was isolated from the cultured pieces of embryo by the guanidinium thiocyanate method of Chomczynski and Sacchi (1987). For all semiquantitative RT-PCR reactions, single-stranded cDNA was synthesised from 1 μg of total cellular RNA. The cDNA synthesis was achieved by using M-MuLV reverse transcriptase (Amersham Pharmacia Biotech). One microgram of total RNA was heated for 10 min at 65°C and then reverse transcribed at 37°C for 1 h using 1 μl Not I-d$(T)_{18}$ (5 μg/μl) diluted 1:25, 1 μl DTT (200 nM) and 5 μl bulk first-strand cDNA reaction mix (murine reverse transcriptase, RNAguard, Rnase/Dnase free BSA, dATP, dCTP, dGTP and dTTP) in a 15-μl reaction. The PCR reaction was carried out using 1 μl of the retrotranscription reaction in a final volume of 50 μl, containing 10× PCR buffer, 1.5 mmol/L $MgCl_2$, 200 μM each dNTPs, 0.2 μM each primer and 1.25 units of Amplitaq DNA polymerase (Applied Biosystems).

For *Cyp26A1* primers were designed using GENbank accession no. AF199462 to generate a 499-bp product, for *Cyp26B1* primers were designed from ChEST239e5 from the BBSRC Chicken EST Project (Boardman et al., 2002) http://www.chick.umist.ac.uk to generate a 385 bp product, for *Cyp26C1* from ChEST1007a3 to generate a 514 bp product. The forward and reverse primers were, respectively, for *Cyp26A1* 5′-GCCTCTCCAACCTTCA-CAAC-3′ and 5′-GTGGCAGACTCCTTCAGCTC-3′; for *Cyp26B1* 5′-TCGGCACTGGCTACCCTCGC-3′ and 5′-

TGGATGTCCCCGATGGAGTT-3′; for *Cyp26C1* 5′-TGCTGCTTTTTTCACCACGG-3′ and 5′-TGTGTCACGGATGCTGTACA-3′.

The β-*actin* gene was co-amplified in each experiment to verify equal amounts of cDNA in the samples. The following forward and reverse primers were used 5′-CGTGACCTGACGGACTACCT′3′ and 5′-CTTCTGCATCCTGTCAGCAA-3′, designed from GENbank accession no. L08165 to generate a 398 bp product. The amplification reaction was initiated by incubation of PCR samples at 94°C for 3 min followed by the cyclic program, at 94°C for 30 s, 58°C for 30 s and 72°C for 1 min for 32 cycles for *Cyp26A1* amplification, at 94°C for 30 s, 58°C for 30 s and 72°C for 1 min for 35 cycles for *Cyp26B1* amplification and 94°C for 30 s, 58°C for 30 s and 72°C for 1 min for 35 cycles for *Cyp26C1* amplification. For each primer set, an increasing linear number of PCR cycles were performed with otherwise fixed conditions to determine the optimal number of cycles to be used. PCR reactions were performed twice and for each gene the products (20 μl) were subjected to electrophoresis in 1% (w/v) agarose gel, visualised by UV after ethidium bromide staining and then sequenced.

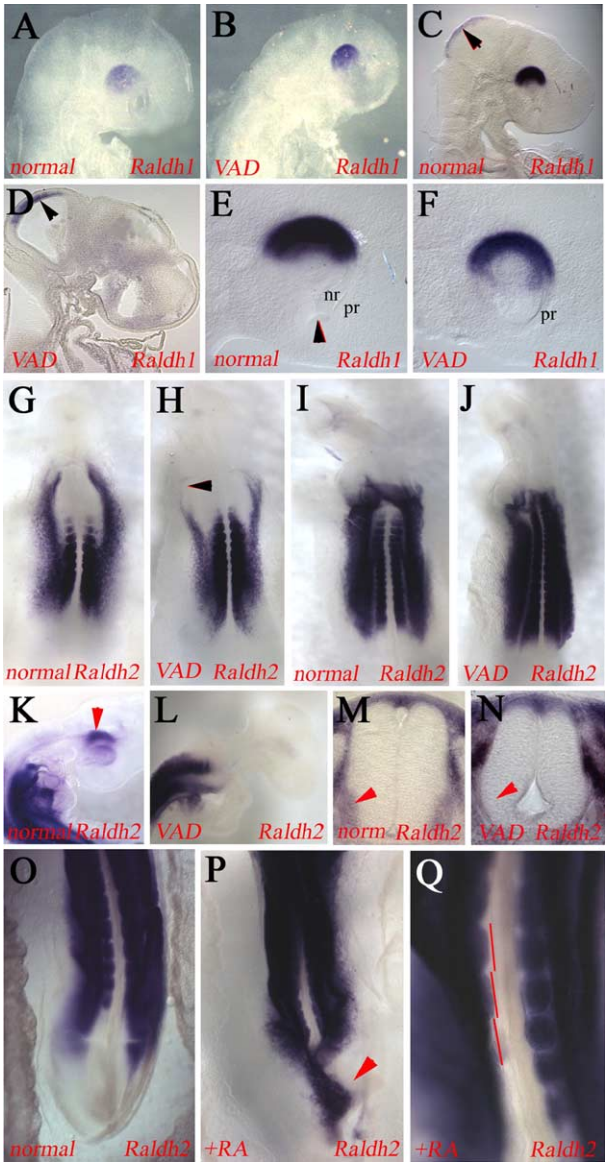

Results

Enzyme regulation in the absence of RA

Raldh1

Both normal and VAD quail embryos show the initial expression of *Raldh1* in the dorsal optic vesicle as chick embryos, beginning at stage 12 (Figs. 1A, B). Thus, the early expression domain of *Raldh1* appears as normal in the absence of RA. This expression in the eye continues in both normal and VAD quail embryos at least until stage 18 (Figs. 1E, F) by which time clear structural differences between the two can be seen. In the normal quail eye (Fig. 1E), the relatively thick layers of neural retina (nr) and pigmented retina (pr) can be seen as well as the choroid fissure making

Fig. 1. *Raldh1* and *Raldh2* expression in normal and VAD quail embryos at various stages of development. (A) Lateral view of the head of a stage 12 normal quail embryo showing *Raldh1* expression in the dorsal half of the eye. (B) Lateral view of the head of a stage 12 VAD quail embryo showing similar *Raldh1* expression in the dorsal half of the eye. (C) Sagittal section of a stage 16 normal embryo showing *Raldh1* expression in the dorsal half of the eye and the roof of the mesencephalon (arrowhead). (D) Sagittal section of a stage 16 normal embryo showing *Raldh1* expression in the ventricular layer of the roof of the mesencephalon (arrowhead). (E) Section of a normal stage 18 eye showing *Raldh1* expression in the dorsal half in both the neural retina (nr) and the pigmented retinal (pr) layers. Arrowhead marks the choroid tissue. (F) In the stage 18 VAD embryo *Raldh1* expression is in the same domains but the retinal layers are very thin and there is no choroid fissure. pr = Pigmented retina. (G) Ventral view of a stage 10 normal embryo showing *Raldh2* expression in the somites from the first somite posteriorly and in the inflow tracts of the heart which extend anteriorly in an arc shape. (H) Ventral view of a stage 10 VAD embryo showing the same *Raldh2* expression in the somites, but a slightly less extensive anterior expression in the heart tracts (arrowhead). (I) Ventral view of a stage 14 normal embryo showing *Raldh2* expression in the somites, lateral plate and in the now more developed heart. (J) Ventral view of a stage 14 VAD embryo showing the same *Raldh2* expression as normal except for a slightly less extensive anterior expression in the heart. (K) Lateral view of the head of a stage 18 normal embryo showing a v-shaped expression domain of *Raldh2* posterior to the eye (red arrowhead) and expression in the dorsal pigmented retina. (L) Lateral view of the head of a stage 18 VAD embryo showing the absence of *Raldh2* expression around and within the eye. (M) Section of a normal stage 20 spinal cord at the forelimb level showing *Raldh2* expression in the developing motor neurons (red arrowhead). (N) Section of a VAD stage 20 spinal cord at the forelimb level showing the absence of *Raldh2* expression in the region of the developing motor neurons (red arrowhead). (O) The posterior end of a normal stage 14 chick embryo showing expression of *Raldh2* in the somites and a small section of unsegmented mesoderm. (P) The posterior end of a stage 14 chick embryo to which a RA bead had been applied overnight. An ectopic growth zone expressing *Raldh2* has been induced which is growing laterally (red arrowhead). (Q) A close-up of the somites of an embryo to which a RA bead had been applied on the left side. The somites are larger than those on the right side, three of which are marked with red lines.

up the characteristic shape of the forming eye. In the VAD eye, the neural retina and pigmented retina layers are much thinner, they are separated by a large gap and there is no choroid fissure (Fig. 1F).

The later domains of *Raldh1* expression described in the chick, namely a region of endoderm and the mesonephros do not appear in the quail. Instead, there is a domain in the mid-sagittal region of the mesencephalon which appears at stage 16 (Fig. 1C, arrowhead). This domain also appears as normal in the VAD embryo; indeed, it seems to be considerably stronger. Sections through such an embryo show expression in the ventricular layers of the mesencephalic neuroepithelium (Fig. 1D). Thus, the absence of RA has little effect upon *Raldh1* expression.

Raldh2

The same expression patterns of *Raldh2* that are seen in the chick are also present in the normal quail embryo and, in general, there is little change in the VAD embryo. Thus, the initial appearance of *Raldh2* in the mesoderm at stage 4 is identical in normal and VAD quails (not shown) and this domain subsequently has an anterior border at the level of the first somite (Figs. 1G, H). The only difference between *Raldh2* expression in the two embryos is that there is a subtle absence of expression in part of the heart inflow tracts (Fig. 1H, arrowhead). This difference remains at later stages where *Raldh2* expression does not extend anteriorly into the heart inflow tracts in VAD embryos (Fig. 1J) as it does in the normals (Fig. 1I). Rather than this abnormal heart expression of *Raldh2* being a cause of the subsequent anatomical heart defects, namely blind ending inflow tracts (Heine et al., 1985), it is more likely that the abnormal expression is a reflection of an earlier patterning defect in the anterior endoderm (Ghatpande et al., 2000).

At later stages of development (stage 18), there are differences in *Raldh2* expression in the head and spinal cord. In normal quails *Raldh2* expression appears in a patch of mesoderm posterior to the eye and in the pigmented retina (Fig. 1K) which also appear in chicks. Both of these domains are absent in the VAD quail embryo (Fig. 1L). A second late domain of expression which is missing is expression in the motor neurons in the spinal cord at limb levels. In chicks and quails, *Raldh2* is expressed in the developing motor neurons (Fig. 1M) and this is absent in the VAD quail (Fig. 1N). This reflects the role of RA in motor neuron induction (Sockanathan and Jessell, 1998) and is mirrored by the down-regulation of other MN markers in the VAD quail spinal cord (Wilson et al., 2004). Thus, three late domains of *Raldh2* do not appear in the absence of RA but there is little alteration in the early domain of *Raldh2.*

Raldh3

As with the previous two enzymes, the initial expression of *Raldh3* is the same as the chick both in the normal quail embryo and the VAD embryo. Thus, Hensen's node expresses *Raldh3* in the normal quail embryo (Fig. 2A) and in the VAD embryo (Fig. 2B). The expression in the surface ectoderm ventral to the forebrain also appears at the appropriate time, stage 9/10, but the domain of expression is much narrower (Figs. 2C, D). This probably reflects a midline defect present in VAD embryos which results in a degree of cyclopia and a loss of the ventral part of the eyes. This narrowness can also be seen at stage 14 when expression is present in the surface ectoderm ventral to the eye (Fig. 2E) which is not so laterally extensive in the VAD embryo (red arrowheads in Figs. 2E, F).

Of the later domains of expression of *Raldh3* in the head, some were normal in VAD quails such as the isthmus (i in Figs. 2G, H, J, K) and the surface ectoderm overlying the ventral half of the eye (Figs. 2G, I, J, L), but the other two domains were missing because of an altered anatomy which had already become apparent. Thus, the expression of *Raldh3* never appears in the ventral half of the eye in VAD

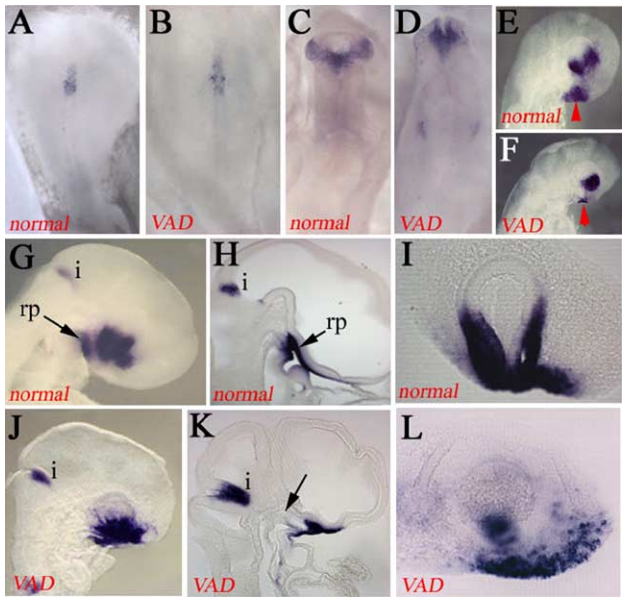

Fig. 2. Expression of *Raldh3* in normal and VAD quail embryos. (A) Normal stage 4 embryos showing expression in Hensen's node. (B) VAD stage 4 embryo showing the same Hensen's node domain as normal. (C) Ventral view of a normal stage 10 embryo showing expression in the ectoderm below the developing forebrain. (D) Ventral view of a stage 10 VAD embryo showing the presence of *Raldh3* expression in the anterior ectoderm, but the domain is much more contracted towards the midline. (E) Lateral view of a stage 12 normal embryo showing expression in the ventral eye and ectoderm (red arrowhead). (F) Lateral view of a stage 12 VAD embryo showing expression in the ventral eye and less extensively in the ectoderm below (red arrowhead). (G) Lateral view of a stage 18 normal head showing expression in the isthmus (i), Rathke's pouch (rp) and in the ventral eye and adjacent ectoderm. (H) Section of an embryo in G, showing expression in the isthmus (i) and Rathke's pouch (rp). (I) Section of a normal stage 18 eye showing expression in both layers of the ventral half of the eye and in the ectoderm below the eye. (J) Expression in the head region of a stage 18 VAD embryo showing expression in the isthmus (i) and the eye region. (K) A section of the embryo in I shows that there is no Rathke's pouch (arrow shows where it ought to be-cf H). (L) Section of a stage 18 VAD eye showing no expression in the ventral part of the eye because there is no tissue there and expression in the overlying ectoderm instead.

embryos (Figs. 2I, L) because that part is missing and neither does it appear in Rathke's pouch because that structure is absent too (rp in Figs. 2G, H vs. arrow in Fig. 2K). Descriptions of these anatomical abnormalities will be reported elsewhere. Thus again, the changes in the expression of this enzyme result from loss of anatomical structures rather than from the absence of its metabolic product.

Cyp26A1

In the normal quail embryo, as in the chick embryo, *Cyp26A1* expression begins at stage 4 in the anterior epiblast and expression then expands posteriorly in two thin lines at the edge of the neural plate where the neural crest will arise and these lines meet at the tail bud within the tail bud mesenchyme (Fig. 3A). In VAD-deficient embryos, the same pattern of expression is seen in the anterior neural plate, but there is no posterior expression of *Cyp26A1* (Fig. 3B). At subsequent stages, the normal anterior expression spreads throughout the forebrain and midbrain and extends posteriorly to the rhombomere 3/4 boundary, whereupon the posterior border regresses anteriorly, leaving a stripe of expression in rhombomere 3 (Fig. 3C, red arrowhead). In VAD embryos, which are lacking the posterior rhombomeres (r4, 5, 6, 7), the same pattern is seen although the expression in rhombomere 3 is weaker and does not extend throughout the dorsoventral extent of the rhombomere (Fig. 3F). Posteriorly at stage 10 in the normal quail, *Cyp26A1* is expressed in the dorsal half of the developing spinal cord (Figs. 3C, D) and the tail bud (Fig. 3C). In VAD embryos, the tail bud expression appears (Fig. 3F), although its time of appearance is delayed, but the spinal cord expression never appears (Figs. 3E, F). There are, therefore, clear differences right from the start of *Cyp26A1* expression at neural plate stages between normal and VAD embryos and these are located in the posterior of the embryo in the presumptive spinal cord region.

Cyp26B1

We have previously described the expression domains of *Cyp26B1* in the normal and VAD quail embryo (Reijntjes et al., 2003), but for the sake of completeness they will be briefly summarised here. In the normal quail embryo, *Cyp26B1* is expressed in the rhombomeres, heart, developing vasculature, eye, hindgut and limb buds (Fig. 3G). In the absence of RA *Cyp26B1* expression in the trunk is strikingly absent in the trunk, in the heart and developing vasculature (Fig. 3H), whereas the rhombomeric expression is maintained (Fig. 3H, hb). Thus from the outset of expression *Cyp26B1*, like *Cyp26A1*, is repressed in the trunk in the absence of RA.

Cyp26C1

Cyp26C1 is a 'head' gene in the normal quail being expressed in the very early anterior mesenchyme, anterior cranial neural crest, specific rhombomeres and discrete regions in the cranial mesenchyme (Reijntjes et al., 2004) (Figs. 3I, K). The major domain which is absent in the VAD embryo is the remaining anterior rhombomeres (the posterior ones are missing) (Figs. 3J, L). Although expression is still present in the head of VAD embryos (Fig. 3J), this is in the cranial mesenchyme adjacent to the

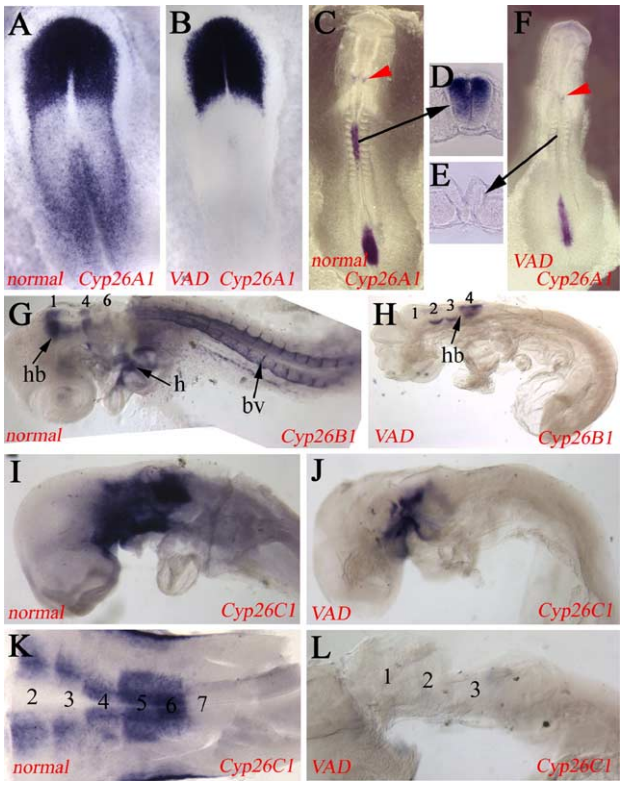

Fig. 3. Expression of the *Cyp* genes in normal and VAD quail embryos. (A) *Cyp26A1* in a normal stage 6 embryo showing expression in the anterior neural plate, lateral edges of the posterior neural plate and the regressing Hensen's node. (B) *Cyp26A1* in a stage 6 VAD embryo. The anterior neural plate expression is normal, but the posterior expression is absent. (C) *Cyp26A1* in a normal stage 10 embryo showing expression in rhombomere 3 (red arrowhead), the anterior neural tube and the tail bud. (D) Section through the embryo in C showing that the neural tube expression of *Cyp26A1* is strongest in the dorsal half. (E) Section through the anterior spinal cord of a stage 10 VAD embryo showing absence of expression of *Cyp26A1*. (F) *Cyp26A1* in a stage 10 VAD embryo showing rhombomere 3 expression (red arrowhead) and tail bud expression, but no anterior spinal cord expression. (G) Lateral view of a stage 16 normal embryo showing expression of *Cyp26B1* in some of the rhombomeres of the hindbrain (hb), the heart (h) and the developing vasculature, particularly between and below the somites (bv). Some of the rhombomeres are marked with numbers. (H) Lateral view of a stage 16 VAD embryo showing expression of *Cyp26B1* remaining in the rhombomeres (numbers) of the hindbrain (hb), but absent from the heart and vasculature. (I) Lateral view of a stage 14 normal embryo showing expression of *Cyp26C1* in some of the rhombomeres of the hindbrain and the surrounding cephalic mesenchyme. (J) Lateral view of a stage 14 VAD embryo showing the absence of expression of *Cyp26C1* the rhombomeres of the hindbrain, but it remains in the surrounding cephalic mesenchyme. (K) Flatmount hindbrain of a stage 22 normal embryo showing discrete expression domains in the individual rhombomeres (numbered) of the hindbrain. (L) Lateral view of a dissected hindbrain of a stage 22 VAD embryo showing absence of expression of *Cyp26C1*. Rhombomeres are numbered.

anterior branchial arches, whereas the expression in the rhombomeres is completely gone (Fig. 3L).

Enzyme regulation in the presence of RA

We next asked whether any of these enzymes could be up-regulated by the administration of excess all-*trans*-RA (tRA) to the embryo. For these experiments, we used local administration on AG 1-X2 beads soaked in 4 mg/ml all-*trans*-RA, a dose which has an in vivo effect of duplicating the chick limb bud. (Tickle et al., 1982). With local administration, we could more carefully analyse potential tissue specific effects and avoid toxicity problems associated with global administration. Beads were applied either adjacent to the head or to the posterior of stage 8–10 embryos and examined after overnight incubation.

Raldh1, 2 and 3

Control beads which had been soaked in DMSO only had no effect on the embryos either in terms of *Raldh* expression or morphology. The application of tRA soaked beads had no effect of the expression of *Raldh1* or *Raldh3*. Regarding *Raldh2*, there was a minority of embryos where a tRA bead beside the head caused a lateral expansion of expression of this enzyme (5 out of 13) because of an anatomical alteration in the structure of

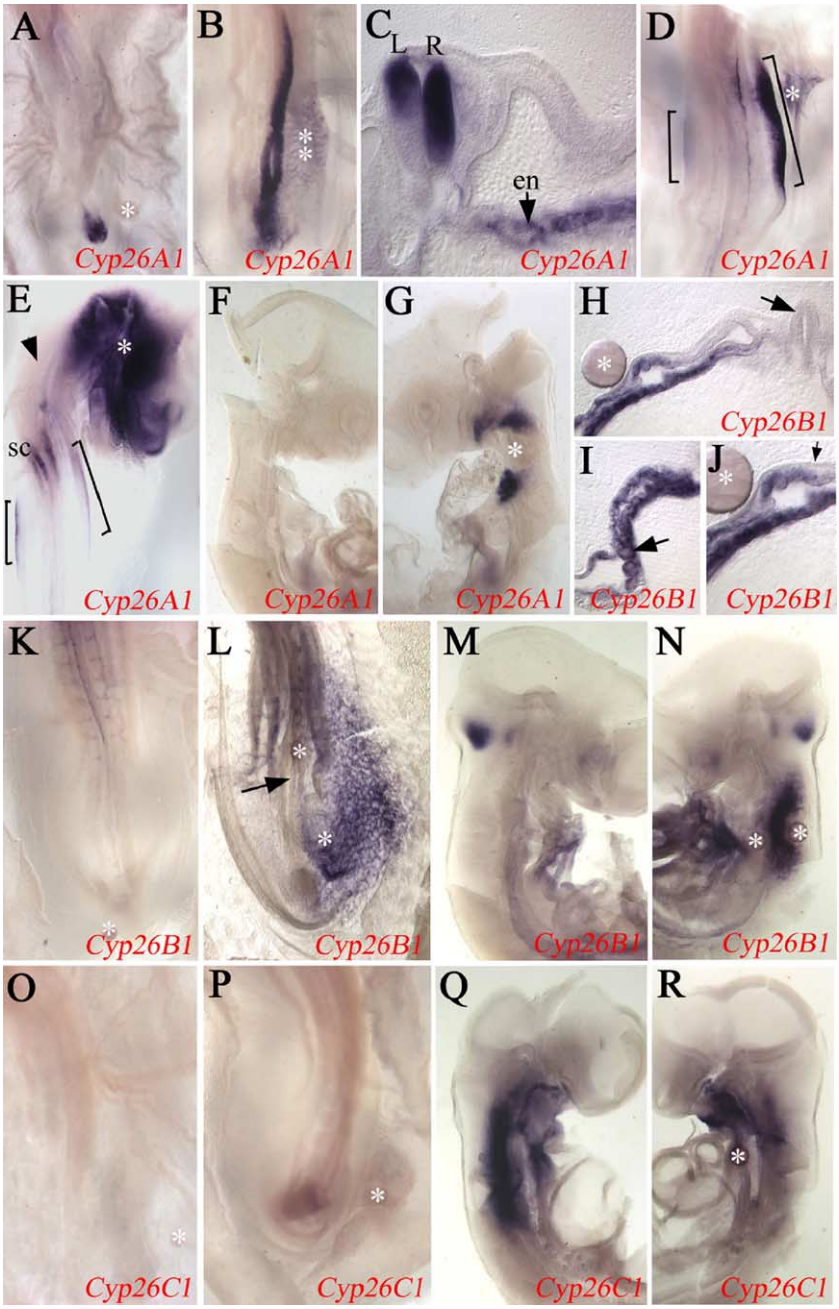

the heart which expresses *Raldh2*. tRA is known to cause cardia bifida when applied to chick embryos and this is what we saw here too (Osmond et al., 1991). When beads were applied to the posterior end of the embryo there was, again, a minority of embryos in which *Raldh2* expression was expanded, also attributable to an alteration in anatomy. One change was a conical or blastemal-like lateral outgrowth from the posterior of the embryo as if the 'stem cell zone' had bifurcated (Figs. 1O, P). The second anatomical effect of tRA was to cause the generation of larger somites on the side to which tRA was applied (Fig. 1Q), the same effect that has been seen in *Xenopus* (Moreno and Kintner, 2004).

Cyp26A1, B1 and C1

Control beads which had been soaked in DMSO only had no effect on the embryos either in terms of *Cyp* expression or morphology. Thus, *Cyp26A1* (Fig. 4A), *Cyp26B1* (Fig. 4K) and *Cyp26C1* (Fig. 4O) were expressed normally in the presence of these control beads.

tRA soaked beads, however, caused a dramatic change in the expression patterns of these enzymes. When placed either at the anterior or posterior end of the embryo *Cyp26A1* was strongly up-regulated by tRA and the up-regulation was tissue-specific. At the posterior end of the embryo *Cyp26A1* was up-regulated in the neural tube and developing vasculature within the splanchnic mesoderm (Figs. 4A vs. B). Sections through such embryos (Fig. 4C) reveal that there was more up-regulation in the neural tube on the right side, the side that the bead was placed (Fig. 4B), than on the left side of the neural tube suggesting a concentration dependent effect. These sections also show up-regulation in the endothelial tubes generating the vasculature, but not in other tissues such as the lateral plate, somites, notochord or epithelium (Fig. 4C). When the beads were placed more anteriorly in the embryo, near the presumptive limb forming regions then *Cyp26A1* was up-regulated in the epithelium overlying the future limb (compare left and right sides of Fig. 4D). In the head region, *Cyp26A1* was strongly up-regulated (Fig. 4E) as there is normally no expression of this gene in the head after neurulation (e.g. Fig. 3C) has been completed. Further analysis of these embryos by dissection and sectioning revealed that the up-regulation was only in the pharyngeal mesoderm (Figs. 4F vs. G) and not in the neuroepithelium of the developing brain. This differential behaviour between cranial and trunk neural tissue can be seen in Fig. 4E where the bead (white asterisk) induced expression in a widespread area of head mesoderm, the epithelium over the presumptive limb bud (bracket in Fig. 4E) and in the anterior end of the spinal cord (sc in Fig. 4E). This spinal cord expression ends at the spinal cord/hindbrain boundary and there is no up-regulation in the hindbrain (black arrowhead in Fig. 4E).

Cyp26B1 was also strongly up-regulated by tRA beads when placed at the posterior end of the embryo in the developing vasculature (Figs. 4K vs. L). Sections through this region (Figs. 4H–J) show that in contrast to *Cyp26A1*, there was no up-regulation of *Cyp26B1* in the neural tube (black arrow in Figs. 4H and 4L), nor in the ectoderm (arrow in Fig. 4J) but only in the endothelial tubes within the splanchnic mesoderm (arrow in Fig. 4I). At the anterior end of the embryo, *Cyp26B1* was up-regulated in the cephalic mesoderm and not in the developing neuroepithelium (Figs. 4M vs. N).

At the posterior end of the normal control embryo *Cyp26C1* is hardly detectable by in situ hybridisation (Fig. 4O) although it is clearly present when assayed by RT-PCR (Fig. 5). The presence of tRA had no significant effect (Fig. 4P). This *Cyp* therefore behaved in a completely different fashion from the other two. Indeed, when tRA beads were placed at the anterior end of the embryo a down-regulation of *Cyp26C1* could be detected in the cephalic mesoderm (Figs. 4Q vs. R).

In order to confirm these differential in situ results we performed PCR experiments using stages 8–10 tail bud or

Fig. 4. Views of stage 12–14 chick embryos to examine the up-regulation of *Cyp26A1*, *B1* or *C1* by all-*trans*-RA applied on a bead. White stars mark the position of the beads. (A) The posterior end of an embryo which received a control bead showing the normal expression of *Cyp26A1*. (B) The posterior end of an embryo which received two RA beads showing strong up-regulation of *Cyp26A1* in the neural tube and in the developing vasculature. (C) A section through the embryo shown in B to reveal the differential up-regulation between the left (L) and right (R) sides of the neural tube, the up-regulation in the endothelial tubes (en) and the lack of up-regulation in the other tissues such as the somites, lateral plate or notochord. (D) An embryo with a bead placed near the head which has up-regulated *Cyp26A1* in the ectoderm overlying the presumptive limb bud on the right side (bracket) compared with its normal expression on the left side (smaller bracket). (E) The anterior end of an embryo showing strong up-regulation of *Cyp26A1* in the head mesenchyme (around the star), no up-regulation in the hindbrain (black arrowhead), up-regulation in the ectoderm overlying the presumptive limb bud (bracket on the right) compared to the left (bracket on the left), and up-regulation in the anterior spinal cord (sc). (F) An embryo such as the one in E which has had the mesenchyme removed to demonstrate that *Cyp26A1* is not up-regulated in the anterior neuroepithelium. (G) An embryo with a less dramatic effect than the one in E showing localised up-regulation of *Cyp26A1* in the cranial mesenchyme. (H) Section through an embryo showing the up-regulation of *Cyp26B1* in the developing vasculature, splanchnic mesoderm and endoderm, but not in the neural tube (arrow) or ectoderm. (I) Higher power of the section in H showing the up-regulation of *Cyp26B1* in the endothelial tubes (arrow). (J) Higher power of the section in H showing the lack of up-regulation of *Cyp26B1* in the ectoderm (arrow) despite the bead (white star) being adjacent to it. (K) The posterior end of an embryo which received a control bead showing the normal expression of *Cyp26B1*. (L) Strong up-regulation of *Cyp26B1* in the developing vasculature after the placement of two RA beads, but no up-regulation in the neural tube (arrow) in contrast to *Cyp26A1*—see B. (M and N) Left (M) and right (N) sides of the head of an embryo which was treated with two RA beads on the right side showing localised induction of *Cyp26B1* in the cephalic mesenchyme and not the neuroepithelium. (O) The posterior end of an embryo which received a control bead showing the virtual lack of expression of *Cyp26C1* in the normal embryo. (P) An embryo which received a RA bead showing a lack of an inductive effect on *Cyp26C1* expression. (Q and R) left (Q) and right (R) sides of the head of an embryo treated with a RA bead on the right side. The left side shows normal expression of *Cyp26C1* in the cranial mesenchyme whereas expression on the right side has been down-regulated around the bead (white star).

brachial arch tissue which had been cultured in 10^{-6} M tRA overnight. Fig. 5, upper panel, confirms that *Cyp26A1* in anterior embryonic tissue was up-regulated by 10^{-6} M tRA (lane 2) compared to untreated control anterior embryonic tissue (lane 1) and that tail bud tissue behaved in the same way (control tail bud tissue lane 3 compared to 10^{-6} M tRA treated tail bud tissue lane 4). Fig. 5 (second panel) shows that *Cyp26B1* was up-regulated in anterior tissue by 10^{-6} M tRA (lane 2 compared to lane 1 untreated tissue) as was *Cyp26B1* in tail bud tissue (untreated tissue lane 3 compared to 10^{-6} M tRA treated lane 4). In contrast, *Cyp26C1* (Fig. 5, third panel) was clearly down-regulated by 10^{-6} M tRA both in anterior tissue (lane 2 compared to untreated control tissue, lane 1) and tail bud tissue (untreated lane 3 compared to 10^{-6} M tRA treated lane 4).

Do the Cyp enzyme products affect the expression of the Cyps?

Since all-*trans*-RA does not affect the expression of the enzymes which synthesise it (the *Raldhs*), we next considered whether the same behaviour was exhibited by the *Cyp* products. The *Cyps* metabolise tRA into various polar compounds including 5,6-*epoxy*-RA, 4-*oxo*-RA, 4-OH-RA and 18-OH-RA (White et al., 1996, 2000; Fujii et al., 1997). We used three of these compounds 5,6-*epoxy*-RA, 4-*oxo*-RA and 4-OH-RA to determine whether they would affect *Cyp* expression in the way that tRA does. As with the tRA experiments, these compounds were administered at a concentration of 4 mg/ml on beads.

4-*oxo*-RA administration produced the same effects as tRA. It strongly up-regulated *Cyp26A1* in the neural tube, tail bud and developing vasculature (Fig. 6A). It strongly up-regulated *Cyp26B1* in the developing vasculature (Fig. 6B) and down-regulated *Cyp26C1* in the cephalic mesoderm (Fig. 6C, red arrowhead). 5,6-*epoxy*-RA behaved the same in up-regulating *Cyp26A1* in the neural tube, epithelium overlying the presumptive limb bud and developing vasculature (Fig. 6D), up-regulating *Cyp26B1* in the developing vasculature (Fig. 6E) and down-regulating *Cyp26C1* in the cephalic mesoderm (Fig. 6F, right side). 4-OH-RA also behaved the same in up-regulating *Cyp26A1* in the neural tube and developing vasculature (Fig. 6G), up-regulating *Cyp26B1* in the developing vasculature (Fig. 6H) and down-regulating *Cyp26C1* in the cephalic mesoderm (Fig. 6I, right side). The only differences between these

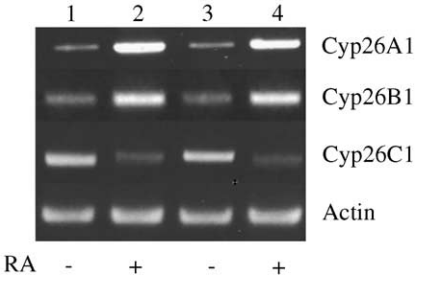

Fig. 5. Semiquantitative RT-PCR experiments on chick tissue from the anterior of the embryo (hindbrain plus associated cranial mesenchyme) and the tail bud cultured in 10^{-6}M tRA overnight. Lane 1, control anterior tissue; lane 2, anterior tissue + 10^{-6}M tRA; lane 3, control tail bud tissue; lane 4, tail bud + 10^{-6}M tRA. The upper panel shows the results for *Cyp26A1* expression with an increase in expression after the addition of tRA; the upper middle panel shows the results for *Cyp26B1* expression with an increase in expression after the addition of tRA; the lower middle panel shows the results for *Cyp26C1* expression with a sharp decrease in expression after the addition of tRA; the lower panel shown no change in the expression of actin with tRA.

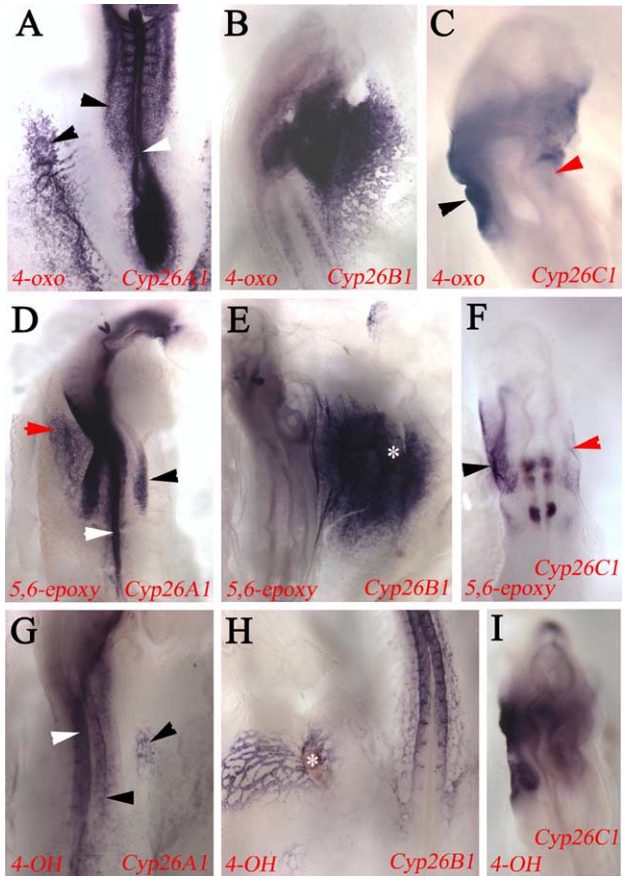

Fig. 6. The effect of 3 Cyp26 metabolites, applied on a bead, on Cyp26 expression. White stars mark the position of the bead. (A) 4-*oxo*-RA strongly induces *Cyp26A1* expression in the developing vasculature (black arrowheads) and in the neural tube (white arrowhead). (B) 4-*oxo*-RA strongly induces *Cyp26B1* in the developing vasculature. (C) 4-*oxo*-RA down-regulates *Cyp26C1* in the cranial mesenchyme on the right side where the bead was placed (red arrowhead) and on the left side the expression is normal (black arrowhead). (D) 5,6-*epoxy*-RA up-regulates *Cyp26A1* expression in the neural tube (white arrowhead), the ectoderm over the presumptive limb bud (black arrowhead) and the developing vasculature (red arrowhead). (E) 5,6-*epoxy*-RA up-regulates *Cyp26B1* expression in the developing vasculature. (F) 5,6-*epoxy*-RA down-regulates *Cyp26C1* in the cranial mesenchyme on the right side (red arrowhead) where the bead was placed and on the left side its expression is normal (black arrowhead). (G) 4-OH-RA up-regulates *Cyp26A1* expression in the neural tube (white arrowhead) and the developing vasculature (black arrowhead). (H) 4-OH-RA up-regulates *Cyp26B1* expression in the developing vasculature. (I) 4-OH-RA down-regulates *Cyp26C1* expression in the cranial mesenchyme on the right side where it was placed and on the left side its expression is normal.

compounds was that 4-OH-RA seemed to have a weaker effect on the levels of up- or down-regulation than the other two compounds.

Which of the RARs does RA act through to alter Cyp expression?

There are three RARs present in higher vertebrate embryos and each of them may act on different target genes. We next used RAR selective agonists to determine which RAR is responsible for altering *Cyp* expression. These compounds have a far higher affinity for either RARα, RARβ or RARγ: CD336 is RARα selective, CD2019 is RARβ selective and CD437 is RARγ selective. They were administered overnight at a concentration of 4 mg/ml on beads as in the previous experiments. The next day, the embryos were examined for *Cyp26A1*, *Cyp26B1* or *Cyp26C1*.

Cyp26A1—the RARα selective compound strongly up-regulated *Cyp26A1* in the neural tube and only weakly in the developing vasculature in 7 out of 9 embryos (Fig. 7A) and weakly induced it in the remaining 2 embryos. The RARβ selective compound produced a very weak up-regulation in the neural tube in 4 out of 9 embryos and had no effect on the remaining 5 embryos (Fig. 7B). The RARγ selective compound generated a very weak alteration of expression in 4 out of 10 embryos and had no effect on the remaining 6 embryos (Fig. 7C). From this, we conclude that *Cyp26A1* is primarily regulated by RARα.

Cyp26B1—the RARα selective compound generated a massive up-regulation of *Cyp26B1* in the developing vasculature in 100% of embryos (Fig. 7D). The RARβ selective compound produced a weak up-regulation in the developing vasculature in 4 out of 9 embryos and had no effect on the remaining 5 embryos (Fig. 7E). The RARγ selective compound had a minor effect on only 1 out of 9 embryos and the remaining 8 embryos showed normal expression. From this, we conclude that *Cyp26B1* is regulated by RARα.

Cyp26C1—the RARα selective compound had an effect in down-regulating *Cyp26C1* expression in the cranial mesenchyme in only 5 out of 11 embryos with the remaining 6 embryos showing normal expression (data not shown). Neither the RARβ selective compound nor the RARγ selective compound had any effect on *Cyp26C1* expression. From this, we conclude that *Cyp26C1* is regulated by RARα.

Are the Cyp products biologically active?

The up-regulation of *Cyp26A1* and *B1* and the down-regulation of *C1* by the *Cyp* products implies that they are potentially biologically active molecules. To test this, we next asked whether they could rescue the VAD quail phenotype. When administered prior to the early somite stage retinol and tRA can completely rescue, all the various system defects in the VAD quail embryos so that they develop normally and survive (Gale et al., 1999). By administering these compounds at a concentration of 4 mg/ml on beads at stages 6–7, we could also rescue VAD quail

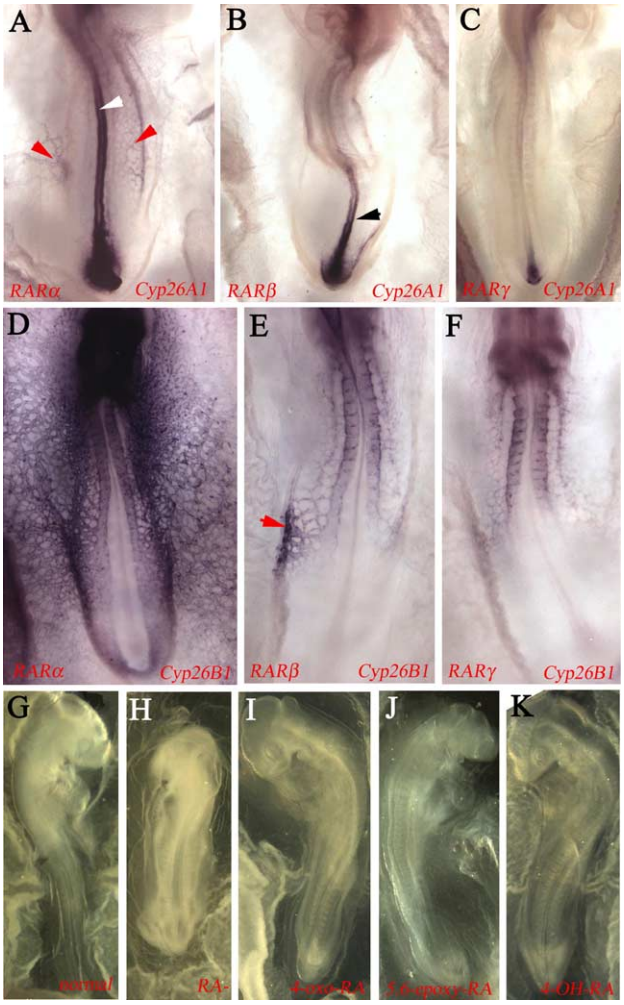

Fig. 7. (A–F) The effect of receptor selective agonists on *Cyp26A1* (A–C) and *Cyp26B1* (D–F) expression. (A) Up-regulation of *Cyp26A1* in the neural tube (white arrowhead) and developing vasculature (red arrowheads) by CD336, a RARα selective compound. Compare with C which shows a normal level of Cyp26A1 expression. (B) Less extensive up-regulation of *Cyp26A1* in the neural tube (black arrowhead) by CD2019, a RARβ selective compound. (C) Lack of effect of CD437, a RARγ compound, on *Cyp26A1* expression. Only the normal expression in the tail bud is apparent. (D) Massive up-regulation of *Cyp26B1* in the developing vasculature by CD336, a RARα selective compound. (E) Less extensive up-regulation of *Cyp26B1* in the developing vasculature (red arrowhead) by CD2019, a RARβ selective compound. (F) Lack of effect of CD437, a RARγ compound, on *Cyp26B1* expression. Only the normal expression in the vasculature in the lateral plate and between the somites is apparent. (G–K) Rescue of the VAD embryo by Cyp products. (G) Normal stage 19 quail embryo. (H) VAD stage 19 quail embryo at the same magnification as G showing how small these embryos are and with their extensive developmental defects—small head, missing posterior hindbrain, small somites, symmetrical heart, absent vitelline veins. (I) VAD embryo treated with beads of 4-*oxo*-RA showing a complete phenotypic rescue. (J) VAD embryo treated with beads of 5,6-epoxy-RA showing a complete phenotypic rescue. (K) VAD embryo treated with beads of 4-OH-RA showing a complete phenotypic rescue.

embryos. Figs. 7G and H show a normal and a VAD quail respectively. The VAD quail is far smaller has a defective neuroepithelium including a missing posterior hindbrain, smaller somites, missing vitelline veins and a symmetrical heart with a blind ending inflow tract. Fig. 7I shows that 4-*oxo*-RA can rescue the VAD quail so that it is indistinguishable from a normal one, as can 5,6-*epoxy*-RA (Fig. 7J) and 4-OH-RA (Fig. 7K).

Discussion

In the work described here, we have studied the regulation of the enzymes which metabolise and catabolise all-*trans*-RA, namely the RALDHs and the CYP26s during avian development. We have performed this firstly, by examining the expression of these enzymes in the absence of RA using the VAD quail model and secondly, by examining their expression in the presence of ectopic tRA. Since RA signals are crucial in the morphogenesis of various embryological systems – the hindbrain, the heart, the eye, the urogenital system, neuronal development in the spinal cord – it is important to understand how such a signal is switched on and off in one location and then on and off in another location.

The RALDHs synthesise RA from retinaldehyde and generate a RA signal that is capable of affecting both the cells that synthesise it and cells in adjacent tissues into which it could diffuse. Since negative feedback is an important aspect of homeostatic control systems we have asked whether tRA affects *Raldh* gene expression in such a fashion. The mechanism of switching off the RA signal is currently thought to involve the Cyp enzymes which catabolise tRA into downstream, and supposedly inactive, metabolites. Since positive feedback is another important aspect of developmental control mechanisms, we have asked whether tRA or the downstream metabolites affect Cyp gene expression.

With regard to the RALDHs we showed that the expression of neither *Raldh1*, *Raldh2* nor *Raldh3* was altered in the absence of RA, that is, their domains of gene expression appeared largely as normal in the VAD quail embryo. Similarly, when a bead which had been soaked in tRA was placed at the anterior or posterior of the chick embryo then ectopic expression of these *Raldh*s was not detected. There were some minor expansions of expression domains caused by the induction of anatomical changes. For example, there was an enlarged domain of *Raldh2* around the heart, caused by the appearance of cardia bifida, which is a known effect of RA application (Osmond et al., 1991). RA application also induced larger somites as has been seen in *Xenopus* (Moreno and Kintner, 2004) and a curious ectopic blastema-like structure at the posterior end of the embryo which seemed to be branching off from the 'stem cell zone'. It is very interesting that excess RA (these results; Moreno and Kintner, 2004) and a lack of RA (Maden et al., 2000) or an inhibition of RA signalling (Moreno and Kintner, 2004) generate larger and smaller somites respectively and in this regard, RA seems to act through a gene called *Thy1* to interact in a negative fashion with FGF signalling in the presomitic mesoderm (Moreno and Kintner, 2004).

This limited effect of RA on *Raldh* expression in embryos is supported by other in vivo and in vitro data. For example, tRA had no effect on *Raldh2* expression in the mouse embryo except at one particular stage when it acted indirectly to down-regulate it (Niederreither et al., 1997). Neither tRA nor 9-*cis*-RA affected *Raldh2* expression in human embryonic kidney cells and the explanation is that no retinoic acid response elements (RARE) or retinoid X response elements could be detected in the promoter upstream from the transcription start site (Wang et al., 2001). However, RA down-regulates *Raldh2* in the zebrafish (Dobbs-McAuliffe et al., 2004) so there may be some species-specific differences in the response of this gene to RA.

In contrast to the *Raldhs*, the *Cyps* were strongly affected both by the absence and presence of excess RA. In the absence of RA, specific domains of the *Cyp*s were missing. For *Cyp26A1*, the domain which localises to the presumptive spinal cord was missing whereas the anterior neural domain in the presumptive forebrain, midbrain and anterior hindbrain and the tail bud domain were normal. This same result is seen in the *Raldh2*$^{-/-}$ mouse (Molotkova et al., 2005). This may contribute to an explanation of the abnormal dorsoventral organisation which is seen in the anterior spinal cord in the absence of RA (Wilson et al., 2004). For *Cyp26B1*, the posterior domain which localises to the developing vasculature and heart is missing, whereas the anterior domain in the rhombomeres appears as normal. This suggests a role for *Cyp26B1* in the development of the cardiovascular system. In zebrafish, however, the development of the common cardinal vein, at least, is abnormal after *Cyp26A1* inhibition (Emoto et al., 2005). For *Cyp26C1*, the rhombomeric domains in the hindbrain were missing whereas the expression in the cranial mesenchyme was normal which suggests a role for *Cyp26C1* in rhombomere patterning. The absence of *Cyp26A1* and *B1* expression in the trunk of the embryo and their induction by RA accords well with the endogenous supply of RA in the embryo which arises in the main from *Raldh2* in the paraxial mesoderm.

Excess tRA induced the strong up-regulation of *Cyp26A1* in the developing vasculature, neural tube, ectoderm over the presumptive limb bud and cranial mesenchyme. The neural tube and limb bud ectoderm are normal sites of expression of *Cyp26A1*, whereas the vasculature is a site of *Cyp26B1* and the cranial mesenchyme is a site of *Cyp26C1* expression. Therefore, each gene seems to be able to be expressed in any of the 'Cyp domains', but not in regions where the Cyps are never expressed, for example, in the somites or in the early

developing brain. Similarly, *Cyp26B1* was ectopically induced in the cranial mesenchyme and developing vasculature, but not elsewhere.

Cyp26C1, however, displayed the opposite effect to the other two *Cyp*s and its expression in the cranial mesenchyme was down-regulated by excess tRA. This surprising differential result was confirmed using RT-PCR-*Cyp26A1* and *B1* are induced by tRA and *Cyp26C1* is repressed. By using synthetic retinoids which show preferences for different retinoic acid receptors (RARs), that is, RAR agonists, we showed that the up-regulation of *Cyp26A1* and *B1* and the down-regulation of *Cyp26C1* operates primarily through RARα. This is not the same result that has been seen in transactivation assays using the three receptors. Of the Cyp products, 4-*oxo*-RA most effectively activated RARα and RARβ, 4-OH-RA was only efficient at activating RARβ and 5,6-*epoxy*-RA most effectively activated RARγ (Idres et al., 2002). Presumably the in vivo situation differs from transactivation assays or the chick RARs behave differently from those of the mouse. The positive and negative feedbacks that we have observed are summarised in Fig. 8.

It is well established that the *Cyp*s are RA-inducible, but their differential behaviour that we have observed here in that *Cyp26C1* was down-regulated by RA is novel. *Cyp26A1* is up-regulated by RA in EC cells (Abu-Abed et al., 1998; Fujii et al., 1997; Ray et al., 1997), various human cell lines (White et al., 1997) in zebrafish (White et al., 1996) and in adult mouse liver, but not in brain (Ray et al., 1997). This is because the upstream region of the promoter contains a RARE which is conserved between zebrafish, mouse and human to which RARγ and RXRα proteins bind (Loudig et al., 2000). In mutant mouse F9 cell lines, there is a decrease in the levels of induction of *Cyp26A1* in a RARγ$^{-/-}$ mutant line and no induction in a RARγ$^{-/-}$/RXRα$^{-/-}$ double mutant line suggesting that these are the nuclear receptors responsible (Abu-Abed et al., 1998). This contrasts with our result of the induction of *Cyp26A1* in the chick embryo with a RARα agonist and the complete inactivity of a RARγ agonist, suggesting a species-specific response. The response of *Cyp26A1* to excess tRA in the mouse embryo is also different to our results in the chick. The anterior of the mouse embryo up-regulates *Cyp26A1* whilst at the posterior end of the embryo it is down-regulated (Fujii et al., 1997) and in the *Xenopus* embryo the same differential phenomenon in different regions of the embryo is seen (Hollemann et al., 1998). Nevertheless, the

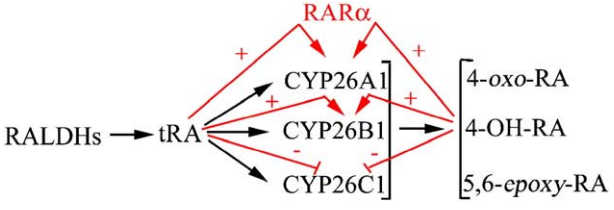

Fig. 8. Summary of the RA synthesis and catabolism pathway (black arrows) and the regulatory interactions we have described (red arrows).

response of *Cyp26A1* in the embryos of both mouse and chick to a lack of RA is identical (Molotkova et al., 2005) so it may be that the elimination of RA is a better test of whether a gene is normally regulated by RA than observing the effects of excess RA.

Cyp26B1 seems to be consistently up-regulated by excess RA in three human cell lines, but not in another (White et al., 2000) as it is in the chick embryo. We suggest that this induction occurs primarily through the RARα receptor. With regard to *Cyp26C1*, the only report of its inducibility is in human keratinocyte cell lines where it is up-regulated (Taimi et al., 2004), whereas we show here that it is down-regulated in the chick embryo.

This induction of *Cyp26A1* and *B1* by their substrate, tRA, which catabolises it into downstream products makes perfect sense in terms of the control of morphogenetic signalling. As considered in Introduction, after a signal has been generated (tRA), there should be a pathway induced to switch it off and so the induction of an enzyme which will destroy tRA and act as a negative regulator seems very logical. The tissues in which this phenomenon occurs are the spinal cord (*Cyp26A1*) and the trunk vasculature and heart (*Cyp26B1*) that is, regions adjacent to *Raldh2* expression. On the other hand, there are certain regions where the Cyp26s are not induced by RA as highlighted by their normal expression in the VAD quail: the anterior neural and tail bud expression of *Cyp26A1* and the rhombomeric expression of *Cyp26B1*. These considerations do not apply, however, to *Cyp26C1* which is down-regulated by tRA and in this case it is acting as a positive regulator.

The action of *Cyp26A1* and *B1* as negative regulators is further reinforced by our findings that at least three of the products of *Cyp* metabolism, 4-*oxo*-RA, 4-OH-RA and 5,6-*epoxy*-RA themselves feedback and up-regulate *Cyp* expression and this up-regulation takes place within exactly the same tissues as found for tRA. This similarity in effect also applies to *Cyp26C1* which is down-regulated in the same tissue by these *Cyp* products. However, the simplicity of this signalling pathway may be somewhat tempered by our observations that these *Cyp* products, 4-*oxo*-RA, 4-OH-RA and 5,6-*epoxy*-RA are themselves biologically active and can act as morphogenetic signals. In our assay of biological activity, we used the VAD quail and showed that these three compounds can fully rescue these embryos which would otherwise have multiple organ defects.

The biological activity of Cyp products has been seen in several other situations. 4-*oxo*-RA alters anteroposterior pattern in the *Xenopus* embryo through its activation of RARβ (Pijnappel et al., 1993; Nikawa et al., 1995) and it can rescue the cardiovascular defects in the VAD quail (Kostetskii et al., 1998). Over-expression of *Cyp26A1* in EC cells should inactivate RA as has been seen many times and thus reduce its differentiating potential, but when these cells are left to differentiate, they turn into neurons (Sonneveld et al., 1999). In mouse skin 4-*oxo*-RA, 4-OH-RA and 5,6-*epoxy*-RA were active in changing the epidermal

thickness (Reynolds et al., 1993) and 4-*oxo*-RA can restore sperm production in vitamin A-deficient mice (Gaemers et al., 1996). In various cell culture lines, these same catabolites inhibited the proliferation and induce differentiation of breast cancer cells (van der Leede et al., 1997; Van Heusden et al., 1998), rhabdomyosarcoma tumour cells (Ramp et al., 1994) and NB4 promyelocytic leukaemia cells (Idres et al., 2001). Interestingly with regard to our results in the chick embryo, the latter effect operates through the RARα receptor. The result of this positive feedback of the two *Cyps*, *A1* and *B1* by their products would lead to the generation of even greater levels of the biologically active catabolic products and presumably a situation of instability. However, it is notable that these results were obtained either using cultured cell lines or with a concentration of retinoids in excess of normal physiological levels. In the mouse embryo, the tail bud defects resulting from the absence of *Cyp26A1* can be rescued by reducing the levels of tRA signalling (Niederreither et al., 2002) and in *Xenopus*, ectopic expression of *Cyp26A1* rescues the embryo from the deleterious effects of excess RA (Hollemann et al., 1998). These results suggest that at least *Cyp26A1* does control the physiological level of tRA. Perhaps therefore in vivo the potentially biologically active Cyp26 products are rapidly further oxidised and do not accumulate to levels which would interfere with tRA signalling.

Acknowledgments

This work was supported by MRC studentships (SR and AB) and the BBSRC (EG and MM). We thank Dr. E. Swindell, Dr. R. Godbout and Dr. F. Grun for RNA probes.

References

Abu-Abed, S.S., Beckett, B.R., Chiba, H., Chithalen, J.V., Jones, G., Metzger, D., Chambon, P., Petkovich, M., 1998. Mouse P450RAI (CYP26) expression and retinoic acid-inducible retinoic acid metabolism in F9 cells are regulated by retinoic acid receptor gamma and retinoid X receptor alpha. J. Biol. Chem. 273, 2409–2415.

Berggren, K., McCaffery, P., Drager, U., Forehand, C.J., 1999. Differential distribution of retinoic acid synthesis in the chicken embryo as determined by immunolocalization of the retinoic acid synthetic enzyme, RALDH-2. Dev. Biol. 210, 288–304.

Blentic, A., Gale, E., Maden, M., 2003. Retinoic acid signalling centres in the avian embryo identified by sites of expression of synthesising and catabolising enzymes. Dev. Dyn. 227, 114–127.

Boardman, P.E., Sanz-Ezquerro, J., Overton, I.M., Burt, D.W., Bosch, E., Fong, W.T., Tickle, C., Brown, W.R., Wilson, S.A., Hubbard, S.J., 2002. A comprehensive collection of chicken cDNAs. Curr. Biol. 12, 1965–1969.

Chambon, P., 1996. A decade of molecular biology of retinoic acid receptors. FASEB J. 10, 940–954.

Chen, Y.-P., Dong, D., Kostetskii, I., Zile, M.H., 1995. Hensen's node from vitamin A-deficient quail embryo induces chick limb bud duplication and retains its normal asymmetric expression of *Sonic hedgehog (Shh)*. Dev. Biol. 173, 256–264.

Chomczynski, P., Sacchi, N., 1987. Single-step method of RNA isolation by acid guanidinium thiocyanate-phenol-chloroform extraction. Anal. Biochem. 162, 156–159.

Cohen, M.M., 2003. The hedgehog signalling network. Am. J. Med. Gen. 123A, 5–28.

de Roos, K., Sonneveld, E., Compaan, B., ten Berge, D., Durston, A.J., van der Saag, P.T., 1999. Expression of retinoic acid 4-hydroxylase (CYP26) during mouse and *Xenopus laevis* embryogenesis. Mech. Dev. 82, 205–211.

Dobbs-McAuliffe, B., Zhao, Q., Linney, E., 2004. Feedback mechanisms regulate retinoic acid production and degradation in the zebrafish embryo. Mech. Dev. 121, 339–350.

Dong, D., Zile, M.H., 1995. Endogenous retinoids in early avian embryo. Biochem. Biophys. Res., 1026–1031.

Duester, G., 1996. Involvement of alcohol dehydrogenase, short-chain dehydrogenase/reductase, aldehyde dehydrogenase, and cytochrome P450 in the control of retinoid signalling by activation of retinoic acid synthesis. Biochemistry 35, 12221–12227.

Duester, G., 2000. Families of retinoid dehydrogenases regulating vitamin A function. Production of visual pigment and retinoic acid. Eur. J. Biochem. 267, 4315–4324.

Eggenschwiler, J.T., Espinoza, E., Anderson, K.V., 2001. Rab23 is an essential negative regulator of the mouse Sonic hedgehog signalling pathway. Nature 412, 194–198.

Emoto, Y., Wada, H., Okamoto, H., Kudo, A., Imai, Y., 2005. Retinoic acid-metabolizing enzyme Cyp26a1 is essential for determining territories of hindbrain and spinal cord in zebrafish. Dev. Biol. 278, 415–427.

Evans, T.M., Ferguson, C., Wainwright, B.J., Parton, R.G., Wicking, C., 2003. Traffic 4, 869–884.

Freeman, M., 2000. Feedback control of intercellular signalling in development. Nature 408, 313–318.

Fujii, H., Sato, T., Kaneko, S., Gotoh, O., Fujii-Kuriyama, Y., Osawa, K., Kato, S., Hamada, H., 1997. Metabolic inactivation of retinoic acid by a novel P450 differentially expressed in developing mouse embryos. EMBO J. 16, 4163–4173.

Gaemers, I.C., van Pelt, A.M., van der Saag, P.T., de Rooij, D.G., 1996. All-trans-4-oxo-retinoic acid: a potent inducer of in vivo proliferation of growth-arrested A spermatogonia in the vitamin A-deficient mouse testis. Endocrinology 137, 479–485.

Gale, E., Zile, M., Maden, M., 1999. Hindbrain respecification in the retinoid-deficient quail. Mech. Dev. 89, 43–54.

Ghatpande, S., Ghatpande, A., Zile, M., Evans, T., 2000. Anterior endoderm is sufficient to rescue foregut apoptosis and heart tube morphogenesis in an embryo lacking retinoic acid. Dev. Biol. 219, 59–70.

Hamburger, V., Hamilton, H.L., 1951. A series of normal stages in the development of the chick embryo. J. Morphol. 88, 49–92.

Heine, U.I., Roberts, A.B., Munoz, E.F., Roche, N.S., Sporn, M.B., 1985. Effects of retinoid deficiency on the development of the heart and vascular system of the quail embryo. Virchow's Arch. B [Cell Pathol.] 50, 135–152.

Hollemann, T., Chen, Y., Grunz, H., Pieler, T., 1998. Regionalized metabolic activity establishes boundaries of retinoic acid signalling. EMBO J. 17, 7361–7372.

Idres, N., Benoit, G., Flexor, M.A., Lanotte, M., Chabot, G.G., 2001. Granulocytic differentiation of human NB4 promyelocytic leukemia cells induced by all-trans retinoic acid metabolites. Cancer Res. 61, 700–705.

Idres, N., Marill, J., Flexor, M.A., Chabot, G.G., 2002. Activation of retinoic acid receptor-dependent transcription by all-trans-retinoic acid metabolites and isomers. J. Biol. Chem. 277, 31491–31498.

Kim, H.H., Bar-Sagi, D., 2004. Modulation of signalling by sprouty: a developing story. Nat. Rev. 5, 441–450.

Kostetskii, I., Yuan, S.-Y., Kostetskaia, E., Linask, K.K., Blanchet, S., Seleiro, E., Michaille, J.-J., Brickell, P., Zile, M., 1998. Initial retinoid requirement for early avian development coincides with retinoid receptor coexpression in the precardiac fields and induction of normal cardiovascular development. Dev. Dyn. 213, 188–198.

Li, H., Wagner, E., McCaffery, P., Smith, D., Andreadis, A., Drager, U.C., 2000. A retinoic acid synthesising enzyme in ventral retina and telencephalon of the embryonic mouse. Mech. Dev. 95, 283–289.

Logan, C.Y., Nusse, R., 2004. The WNT signalling pathway in development and disease. Ann. Rev. Cell Dev. Biology 20, 781–810.

Loudig, O., Babichuk, C., White, J., Abu-Abed, S., Mueller, C., Petkovich, M., 2000. Cytochrome P450RAI(CYP26) promoter: a distinct composite retinoic acid response element underlies the complex regulation of retinoic acid metabolism. Mol. Endocrinol. 14, 1483–1497.

MacLean, G., Abu-Abed, S., Dolle, P., Tahayato, A., Chambon, P., Petkovich, M., 2001. Cloning of a novel retinoic-acid metabolizing cytochrome P450, Cyp26B1, and comparative expression analysis with Cyp26A1 during early murine development. Mech. Dev. 107, 195–201.

Maden, M., Graham, A., Zile, M., Gale, E., 2000. Abnormalities of somite development in the absence of retinoic acid. Int. J. Dev. Biol. 44, 151–159.

McCaffery, P., Tempst, P., Lara, G., Drager, U.C., 1991. Aldehyde dehydrogenase is a positional marker in the retina. Development 112, 693–702.

Mic, F.A., Molotkov, A., Fan, X., Cuenca, A.E., Duester, G., 2000. RALDH3, a retinaldehyde dehydrogenase that generates retinoic acid, is expressed in the ventral retina, otic vesicle and olfactory pit during mouse development. Mech. Dev. 97, 227–230.

Molotkova, N., Molotkov, A., Sirbu, O., Duester, G., 2005. Requirement of mesodermal retinoic acid generated by Raldh2 for posterior neural transformation. Mech. Dev. 122, 145–155.

Moreno, T.A., Kintner, C., 2004. Regulation of segmental patterning by retinoic acid signaling during *Xenopus* somitogenesis. Dev. Cell 6, 205–218.

Moss, J.B., Xavier-Neto, J., Shapiro, M.D., Nayeem, S.M., McCaffery, P., Drager, U.C., Rosenthal, N., 1998. Dynamic patterns of retinoic acid synthesis and response in the developing mammalian heart. Dev. Biol. 199, 55–71.

Munoz-Sanjuan, I., Brivanlou, A.H., 2002. Neural induction, the default model and embryonic stem cells. Nat. Rev. 3, 271–280.

Niederreither, K., McCaffery, P., Drager, U.C., Chambon, P., Dolle, P., 1997. Restricted expression and retinoic acid-induced downregulation of the retinaldehyde dehydrogenase type 2 (RALDH-2) gene during mouse development. Mech. Dev. 62, 67–78.

Niederreither, K., Abu-Abed, S., Schubaur, B., Petkovich, M., Chambon, P., Dollé, P., 2002. Genetic evidence that oxidative derivatives of retinoic acid are not involved in retinoid signaling during mouse development. Nat. Genet. 31, 84–88.

Nikawa, T., Schulz, W.A., van den Brink, C.E., Hanusch, M., van der, S.P., Stahl, W., Sies, H., 1995. Efficacy of all-trans-beta-carotene, canthaxanthin, and all-trans-, 9-cis-, and 4-oxoretinoic acids in inducing differentiation of an F9 embryonal carcinoma RAR beta-lacZ reporter cell line. Arch. Biochem. Biophys. 316, 665–672.

Osmond, M.K., Butler, A.J., Voon, F.C.T., Bellairs, R., 1991. The effects of retinoic acid on heart formation in the early chick embryo. Development 113, 1405–1417.

Pijnappel, W.W.M., Hendricks, H.F.J., Folkers, G.E., van den Brink, C.E., Dekker, E.J., Edelenbosch, C., van der Saag, P.T., Durston, A.J., 1993. The retinoid ligand 4-oxo-retinoic acid is a highly active modulator of positional specification. Nature 366, 340–344.

Ramp, U., Gerharz, C.D., Eifler, E., Biesalski, H.K., Gabbert, H.E., 1994. Effects of retinoic acid metabolites on proliferation and differentiation of the clonal rhabdomyosarcoma cell line BA-HAN-1C. Biol. Cell 81, 31–37.

Ray, W.J., Bain, G., Yao, M., Gottlieb, D.I., 1997. CYP26, a novel mammalian cytochrome P450, is induced by retinoic acid and defines a new family. J. Biol. Chem. 272, 18702–18708.

Reijntjes, S., Gale, E., Maden, M., 2003. Expression of the retinoic acid catabolising enzyme CYP26B1 in the chick embryo and its regulation by retinoic acid. Gene Expr. Patterns 3, 621–627.

Reijntjes, S., Gale, E., Maden, M., 2004. Generating gradients of retinoic acid in the chick embryo: Cyp26C1 expression and a comparative analysis of the Cyp26 enzymes. Dev. Dyn. 230, 509–517.

Reynolds, N.J., Fisher, G.J., Griffiths, C.E., Tavakkol, A., Talwar, H.S., Rowse, P.E., Hamilton, T.A., Voorhees, J.J., 1993. Retinoic acid metabolites exhibit biological activity in human keratinocytes, mouse melanoma cells and hairless mouse skin in vivo. J. Pharmacol. Exp. Ther. 266, 1636–1642.

Schneider, R.A., Hu, D., Rubenstein, J.L.R., Maden, M., Helms, J.A., 2001. Local retinoid signalling coordinates forebrain and facial morphogenesis by maintaining FGF8 and SHH. Development 128, 2755–2767.

Sockanathan, S., Jessell, T.M., 1998. Motor neuron-derived retinoid signalling specifies the subtype identity of spinal motor neurons. Cell 94, 503–514.

Sonneveld, E., van den Brink, C.E., Tertoolen, L.G.J., van der Burg, B., van der Saag, P.T., 1999. Retinoic acid hydroxylase (CYP26) is a key enzyme in neuronal differentiation of embryonal carcinoma cells. Dev. Biol. 213, 390–404.

Swindell, E.C., Thaller, C., Sockanathan, S., Petkovich, M., Jessell, T.M., Eichele, G., 1999. Complementary domains of retinoic acid production and degradation in the early chick embryo. Dev. Biol. 216, 282–296.

Tahayato, A., Dolle, P., Petkovich, M., 2003. Cyp26C1 encodes a novel retinoic acid-metabolizing enzyme expressed in the hindbrain, inner ear, first branchial arch and tooth buds during murine development. Gene Exp. Patterns 3, 449–454.

Taimi, M., Helvig, C., Wisniewski, J., Ramshaw, H., White, J.A., Amad, M., Korczak, B., Petkovich, M., 2004. A novel human cytochrome P450, CYP26C1, involved in metabolism of 9-cis and all-trans isomers of retinoic acid. J. Biol. Chem. 279, 77–85.

Tickle, C., Alberts, B., Wolpert, L., Lee, J., 1982. Local application of retinoic acid to the limb bond mimics the action of the polarizing region. Nature 296, 564–566.

Twal, W.O., Roze, L., Zile, M.H., 1995. Anti-retinoic acid monoclonal antibody localizes all-trans-retinoic acid in target cells and blocks normal cardiovascular development. Dev. Biol. 168, 225–234.

van der Leede, B.M., van den Brink, C.E., Pijnappel, W.W., Sonneveld, E., van der Saag, P.T., van der, B.B., 1997. Autoinduction of retinoic acid metabolism to polar derivatives with decreased biological activity in retinoic acid-sensitive, but not in retinoic acid-resistant human breast cancer cells. J. Biol. Chem. 272, 17921–17928.

Van Heusden, J., Wouters, W., Ramaekers, F.C., Krekels, M.D., Dillen, L., Borgers, M., Smets, G., 1998. All-trans-retinoic acid metabolites significantly inhibit the proliferation of MCF-7 human breast cancer cells in vitro. Br. J. Cancer 77, 26–32.

Wang, X., Sperkova, Z., Napoli, J.L., 2001. Analysis of mouse retinal dehydrogenase type 2 promoter and expression. Genomics 74, 245–250.

White, J.A., Guo, Y.D., Baetz, K., Beckett-Jones, B., Bonasoro, J., Hsu, K.E., Dilworth, F.J., Jones, G., Petkovich, M., 1996. Identification of the retinoic acid-inducible all-trans-retinoic acid 4-hydroxylase. J. Biol. Chem. 271, 29922–29927.

White, J.A., Beckett-Jones, B., Guo, Y.D., Dilworth, F.J., Bonasoro, J., Jones, G., Petkovich, M., 1997. cDNA cloning of human retinoic acid-metabolizing enzyme (hP450RAI) identifies a novel family of cytochromes P450. J. Biol. Chem. 272, 18538–18541.

White, J.A., Ramshaw, H., Taimi, M., Stangle, W., Zhang, A., Everingham, S., Creighton, S., Tam, S.P., Jones, G., Petkovich, M., 2000. Identification of the human cytochrome P450, P450RAI-2, which is predominantly expressed in the adult cerebellum and is responsible for all-trans-retinoic acid metabolism. Proc. Natl. Acad. Sci. U. S. A. 97, 6403–6408.

Wilson, L., Gale, E., Chambers, D., Maden, M., 2004. Retinoic acid and the control of dorsoventral patterning in the avian spinal cord. Dev. Biol. 269, 433–446.

Zhao, D., McCaffery, P., Ivins, K.J., Neve, R.L., Hogan, P., Chin, W.W., Drager, U.C., 1996. Molecular identification of a major retinoic acid-synthesising enzyme, a retinaldehyde-specific dehydrogenase. Eur. J. Biochem. 240, 15–22.